JBC RESEARCH ARTICLE

Cardiac myosin-binding protein C interaction with actin is inhibited by compounds identified in a high-throughput fluorescence lifetime screen

Received for publication, March 4, 2021, and in revised form, May 19, 2021 Published, Papers in Press, May 28, 2021,
https://doi.org/10.1016/j.jbc.2021.100840

Thomas A. Bunch[1], Piyali Guhathakurta[2], Victoria C. Lepak[1], Andrew R. Thompson[2], Rhye-Samuel Kanassatega[1], Anna Wilson[2], David D. Thomas[2], and Brett A. Colson[1,*]

From the [1]Department of Cellular & Molecular Medicine, University of Arizona, Tucson Arizona, USA; and [2]Department of Biochemistry, Molecular Biology, and Biophysics, University of Minnesota, Minneapolis, Minnesota, USA

Edited by Enrique De La Cruz

Cardiac myosin-binding protein C (cMyBP-C) interacts with actin and myosin to modulate cardiac muscle contractility. These interactions are disfavored by cMyBP-C phosphorylation. Heart failure patients often display decreased cMyBP-C phosphorylation, and phosphorylation in model systems has been shown to be cardioprotective against heart failure. Therefore, cMyBP-C is a potential target for heart failure drugs that mimic phosphorylation or perturb its interactions with actin/myosin. Here we have used a novel fluorescence lifetime-based assay to identify small-molecule inhibitors of actin-cMyBP-C binding. Actin was labeled with a fluorescent dye (Alexa Fluor 568, AF568) near its cMyBP-C binding sites; when combined with the cMyBP-C N-terminal fragment, C0-C2, the fluorescence lifetime of AF568-actin decreases. Using this reduction in lifetime as a readout of actin binding, a high-throughput screen of a 1280-compound library identified three reproducible hit compounds (suramin, NF023, and aurintricarboxylic acid) that reduced C0-C2 binding to actin in the micromolar range. Binding of phosphorylated C0-C2 was also blocked by these compounds. That they specifically block binding was confirmed by an actin-C0-C2 time-resolved FRET (TR-FRET) binding assay. Isothermal titration calorimetry (ITC) and transient phosphorescence anisotropy (TPA) confirmed that these compounds bind to cMyBP-C, but not to actin. TPA results were also consistent with these compounds inhibiting C0-C2 binding to actin. We conclude that the actin-cMyBP-C fluorescence lifetime assay permits detection of pharmacologically active compounds that affect cMyBP-C-actin binding. We now have, for the first time, a validated high-throughput screen focused on cMyBP-C, a regulator of cardiac muscle contractility and known key factor in heart failure.

Cardiac myosin-binding protein C (cMyBP-C, Fig. 1) has been identified as a therapeutic target for systolic or diastolic dysfunction in heart failure and cardiomyopathy. cMyBP-C may contribute to heart failure due to hypertrophic cardiomyopathy (HCM) or dilated cardiomyopathy (DCM).

HCM is a common heart disease, affecting around 1:500 individuals, for which there are few therapeutic treatments (1). In HCM the heart typically becomes enlarged, hypercontractile, and unable to relax effectively. The systolic contraction is preserved, but diastolic relaxation is diminished. HCM is associated with heart failure, arrhythmias, and cardiac death at any age. The primary cause of HCM is most often a missense mutation in one of several sarcomeric proteins or the truncation of cMyBP-C. In addition to cMyBP-C, the sarcomeric proteins associated with HCM include those associated with the thick (myosin) and thin (actin) filaments, including myosin, troponin, tropomyosin, leiomodin, and titin.

DCM results from missense mutations in some of the same sarcomeric genes as for HCM (but not cMyBP-C truncations) as well as Z-disk proteins (2). DCM can also be caused by mutations in nonsarcomeric genes, such as those encoding proteins of the nucleus, ion channels, and cytoskeleton (3). Any one of these mutations leads to dilation of the ventricular chambers and defects in systolic contraction.

Numerous studies have demonstrated that increasing or decreasing PKA-mediated phosphorylation of cMyBP-C allows for tuning cardiac contraction and relaxation through phosphorylation-sensitive interactions with actin and myosin. These interactions and their effects are complex, and it is not yet fully understood how they are integrated. Binding to actin is proposed to activate the thin filament in low calcium conditions by repositioning tropomyosin to the unblocked position, thereby stimulating contraction (4, 5). Binding to actin has also been observed to shift F-actin to a more ordered state, similar to the effect of myosin binding to actin (6, 7). This ordered state may also promote myosin binding to actin. During relaxation, cMyBP-C bound to actin is proposed to generate a drag on the sliding of the filaments, thereby slowing relaxation (8–10). cMyBP-C is also necessary for complete relaxation during diastole (11). cMyBP-C binding to myosin heads has been reported to favor the super-relaxed state, keeping them inactive (12, 13). Phosphorylation, by decreasing and modifying interactions with the thin and thick filaments (7, 14–17), can therefore have multiple effects: reduce activation at low calcium (18), increase relaxation by preventing the drag imposed by

* For correspondence: Brett A. Colson, bcolson@arizona.edu.

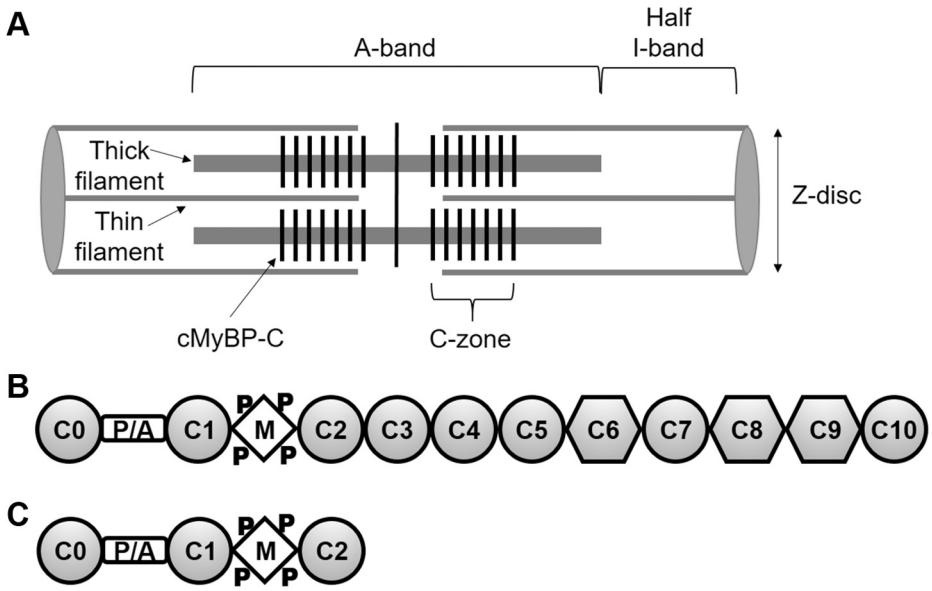

Figure 1. cMyBP-C organization. *A*, the sarcomere spans from Z-disc to Z-disc with the A-band containing thick filaments and the I-band containing actin filaments. Force is generated by myosin and actin in the thin/thick filament overlap portion of the A-band. cMyBP-C molecules (*black vertical stripes*) are present in the C-zones toward the center of the A-band. The C-zones overlap with thin filaments (except at very long sarcomere lengths). *B*, full-length cMyBP-C domains C0 through C10. Ig-like domains are shown as circles and fibronectin type-III domains are shown as hexagons. *C*, N-terminal domains C0 through C2 (C0-C2), containing the proline/alanine-rich linker (P/A) and the M-domain (M) that contains phosphorylation sites (P).

cMyBP-C binding to actin (10, 19) to enhance relaxation (20), decrease myosin binding due to increased disorder in actin (6, 7), and increase myosin binding and contraction by releasing myosin heads from the super-relaxed state (13, 21). Recent work by us (22) and others (23) suggests that phosphorylation causes a rearrangement of N-terminal cMyBP-C structure that reduces binding to actin and myosin to modulate contraction and relaxation. Decreases in phosphorylation of cMyBP-C have been observed in heart failure and HCM patients, including those affected by mutations in cMyBP-C and sarcomeric proteins other than cMyBP-C (24, 25). Therefore, targeting cMyBP-C with drugs that mimic phosphorylation and that modulate its binding to actin or myosin is a promising approach to improve cardiac muscle function in heart failure and cardiomyopathy. Recently, cardiac-specific, small-molecule effectors of myosin have been developed to activate or inhibit cardiac muscle contraction in heart failure and HCM (26, 27). While some ongoing human clinical trials are promising, alternative strategies, such as targeting cardiac-specific actomyosin accessory proteins (*i.e.*, cMyBP-C) may prove valuable as well. Despite strong evidence implicating cMyBP-C as an ideal target for therapy, no cMyBP-C small-molecule modulator has been identified. A critical barrier to progress in this area is that high-throughput screening (HTS) assays based on cMyBP-C functional activities have not been available.

Current *in vitro* actin or myosin-binding assays, such as cosedimentation, are labor-intensive and low-throughput, limited in the number of samples that can be tested. Recent development of fluorescence lifetime plate readers (28) now allows for high-throughput (~3 min/microplate), high-precision (picoseconds for lifetime and nanometers for distances) assays that are scalable (in-plate, 1536-well plates, detection) and reduce labor.

We recently developed a fluorescence lifetime HTS assay for detecting the interaction of F-actin with N-terminal cMyBP-C domains C0-C2 (15). The time-resolved fluorescence (TR-F) assay reported a significant reduction in lifetime of IAEDANS attached to actin at Cys-374 when incubated with C0-C2. This reduction was concentration-dependent and correlated with actin binding of C0-C2 as measured by cosedimentation assays. The high precision of the TR-F assay was demonstrated by resolving significant changes in binding due to phosphorylation and mutations relevant to HCM and function.

In the present study, we have used this TR-F assay, using a fluorescence lifetime plate reader (see Experimental procedures) to screen the Library of Pharmacologically Active Compounds (LOPAC). We selected this library because it is a diverse collection of 1280 pharmacologically active compounds that includes all major drug target classes, inhibitors, pharma-developed tools, and approved drugs. To reduce interference with compounds exhibiting fluorescence at shorter wavelengths (29, 30), we labeled actin with the red-shifted fluorescent dye, Alexa Fluor 568 (AF568), which was excited by a 532-nm microchip laser. This screen reproducibly identified three compounds that appeared to reduce MyBP-C binding to actin in the micromolar range. We then tested these "Hit" compounds for dose dependence in the TR-F assay and further evaluated their efficacy in biochemical and biophysical secondary assays. To verify compound–target engagement, isothermal titration calorimetry (ITC) determined the micromolar affinity of the three Hit compounds to cMyBP-C. Transient phosphorescence anisotropy (TPA) provided further proof that the Hit compounds did not bind to actin and that they inhibited C0-C2–actin interactions. Finally, we developed a novel TR-FRET assay as an alternative method to monitor C0-C2

binding to actin. We used this TR-FRET assay to confirm the effects of the identified Hits on actin binding.

This is the first HTS assay to identify compounds that specifically bind to human cMyBP-C and modulate its interactions with actin. The results of this study provide proof-of-concept validation for the TR-F assay in identifying effective cMyBP-C-specific modulators of actomyosin function. This new tool will be valuable in the development of new therapies for cardiac muscle diseases.

Results

Actin-cMyBP-C TR-F biosensor

We have previously described a TR-F based C0-C2–actin-binding assay utilizing IAEDANS-labeled actin. The lifetime, τ, of IAEDANS attached to actin was reduced upon C0-C2 binding. This provided a rapid way to monitor binding in a multiwell plate format conducive to screening libraries of compounds that modulate actin-cMyBP-C binding (15). Unfortunately, a high percentage of compounds fluoresce at the shorter wavelength used to excite IAEDANS (8). To decrease this problem, we tested the TR-F response of C0-C2 binding to actin, where the actin was labeled with probes that are excited at longer wavelengths, permitting the use of a longer-wavelength laser (29).

TR-F decays of Alexa Fluor 546 (AF546) and Alexa Fluor 568 (AF568)-labeled actin in the presence of cMyBP-C N-terminal fragment (C0-C2) (Fig. 2*A*) were analyzed by one-exponential fitting (see Experimental procedures) to determine fluorescence lifetime (Fig. 2, *B* and *C* and Fig. S1*A*). Both probes on actin showed lifetime decreased with increasing C0-C2 concentration, indicating binding. This effect was reduced with phosphorylated C0-C2, indicating less binding (Fig. 2*D*). As AF568 showed a greater change in lifetime upon C0-C2 binding to F-actin, we used this probe for the HTS screen. Analysis of TR-F binding curves with 1 μM AF568-actin revealed that at 2 μM C0-C2 the lifetime is highly sensitive to phosphorylation by PKA (Fig. 2*D*). Since our goal was to detect compounds that show differences in binding similar to those detected upon PKA phosphorylation, we selected these concentrations of AF568-actin (1 μM) and C0-C2 (2 μM) to perform the screen. From cosedimentation assays (15), we know that these correspond to binding ratios of ∼1:7 C0-C2:actin, which is similar to that found in the muscle sarcomere.

High-throughput screening of LOPAC library to identify compounds that modulate actin-cMyBP-C TR-F

We performed HTS using the LOPAC library (see Experimental procedures). The screen was performed in duplicate with two different preparations of AF568-actin and C0-C2 samples. Each screen tested the effect of the compounds on the lifetime of AF568-actin and the effect of the compounds on the lifetime of AF568-actin in the presence of C0-C2 (AF568-

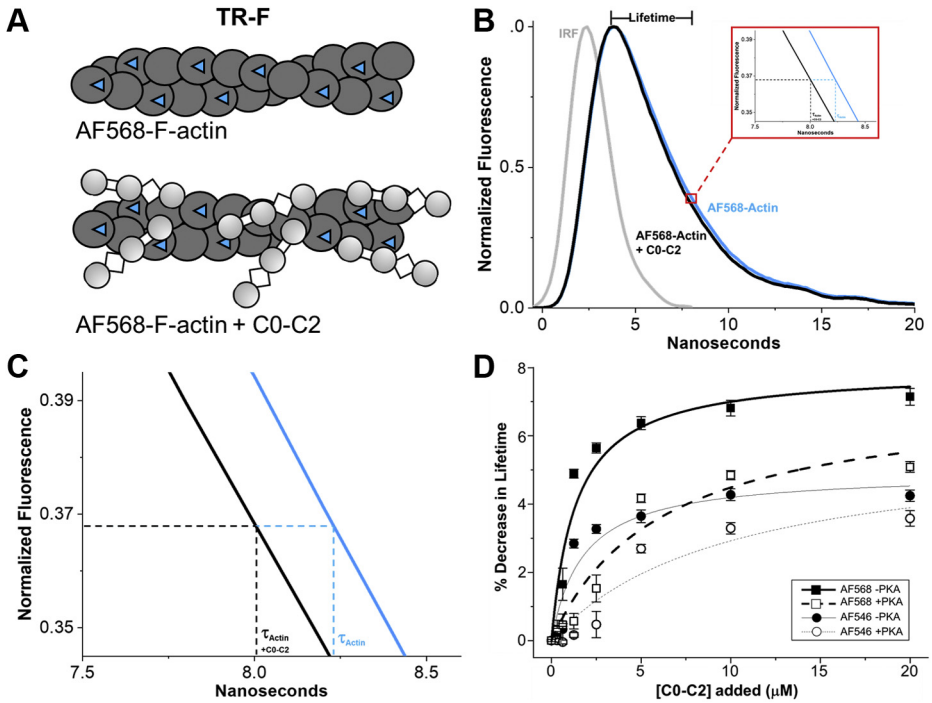

Figure 2. TR-F of AF568-F-actin is reduced upon C0-C2 binding. *A*, cartoon rendering of F-actin with AF568 (*blue triangles*) attached to ∼50% of monomers (AF568-actin, *dark gray circles*) and the same upon binding of C0-C2. *B*, fluorescence waveforms of AF568-actin (*blue line*) and the same in the presence of 20 μM C0-C2 (*black line*) normalized to maximal fluorescence intensity (waveforms without normalization can be found in Fig. S1*A*). Lifetime (τ) is the time at which the peak fluorescence decays to ∼0.37 (1/e). *Red box* shows expansion of the *x*-axis near the lifetimes of the AF568- actin. *C*, further expansion of the *red box area* in *B*. Note that τ is the time to the decay to 1/e (∼8–8.5 ns) less the time of the rising phase of the waveform (∼4 ns), and so measured τ values are actually ∼4–4.5 ns. *D*, comparison of AF546- (*circles, thin gray lines*) and AF568-actin (*squares, thick black lines*) binding curves for 0–20 μM C0-C2 without (*solid circles/squares, solid lines*) and with PKA phosphorylation (*open circles/squares, dashed lines*). Levels of actin labeled were 65%, 40%, and 34% for AF568 (three separate preparations) and 87% and 28% for AF546 (two separate preparations). Values are the % decrease in lifetime of each of the two probes in the presence of 0–20 μM C0-C2 compared with actin alone (n = 15 for AF568; n = 9 for AF546).

actin:C0-C2). The Z' factor for this screen was calculated as 0.5 ± 0.1 using DMSO-only controls, validating the robustness of this HTS assay (see Experimental procedures). Compounds that altered the lifetime of AF568-actin alone by more than 4 standard deviations (SD) of the mean of controls (no compound) were excluded from the analysis of the AF568-actin:C0-C2 results. This removed 210 and 106 compounds from the first and second screen, respectively. The change in lifetime of AF568-actin due to effects of each compound on AF568-actin:C0-C2 complex was determined by subtracting the effects of each compound on AF568-actin alone from the effects on AF568-actin:C0-C2. Since C0-C2 binding reduced AF568-actin lifetime, compounds interfering with C0-C2 binding to actin increased the lifetime of AF568-actin:C0-C2. Positive changes from both screens were sorted, ranked, and compared. The top 25 compounds revealed three compounds (designated "Hits") in common and 22 that were not repeatable (Tables S1 and S2). Two additional suboptimal (explained in Experimental procedures) screens of the same library also yielded only these three Hit compounds in the top 25 preliminary hits. Each of these had 22 false positives that were not identified in any of the other screens (Tables S3 and S4). Thus, the Hit rate was 0.23%.

Suramin showed the greatest effect, with an average change in lifetime that was 6.5 SD above the median (of all compounds not excluded due to large effects on AF568-actin alone); NF023 (a suramin analog) was 3.8 SD above the median; and aurintricarboxylic acid (ATA) was 3.0 SD above the median. These three Hit compounds were tested further in orthogonal assays.

TR-F dose–response assay

Using the same conditions as in the primary screen, we determined the concentration dependence of each of the three Hit compounds on the AF568-actin lifetime effects. As observed in the screen, all three Hit compounds had little effect on AF568-actin alone (Fig. 3*A*). C0-C2 reduced the lifetime of AF568, and all three Hit compounds, in a concentration-dependent manner, returned AF568 to the lifetime observed for AF568-actin alone (Fig. 3*A*). This is consistent with all three Hit compounds inhibiting C0-C2 binding to actin. The apparent EC_{50} (concentration of compound needed for half-maximal effect) of the Hit compounds as measured by TR-F is 5–20 μM (Fig. 3, Table 1). In a separate dose–response assay utilizing 3 μM C0-C2, we compared the effects of the compounds on nonphosphorylated and phosphorylated C0-C2. When AF568-actin was bound to C0-C2 phosphorylated by PKA, a decreased lifetime of AF568 was observed (though the decrease was smaller than with nonphosphorylated C0-C2) and all three Hit compounds again returned AF568 lifetime to that of AF568-actin alone (Fig. 3*B*). In the second dose-response assay, 3 μM instead of 2 μM C0-C2 was used in the second dose–response assay so that effects of compounds on phosphorylated C0-C2 could be readily detected, as phosphorylation of C0-C2 itself (in the absence of compounds) reduces binding to actin.

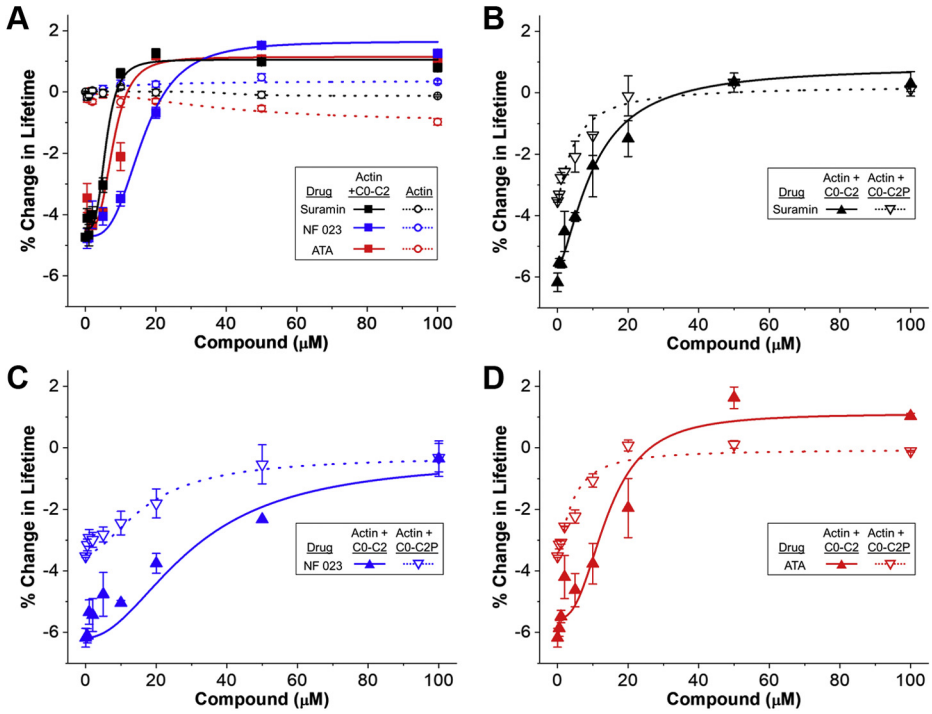

Figure 3. Concentration–response curves for Hit compounds on AF568-actin-C0-C2 TR-F. Percent change in AF568 Lifetime (relative to AF568-actin alone) for (*A*) 1 μM AF568-actin (*open circles, dotted lines*) and 1 μM AF568-actin with 2 μM C0-C2 (*solid squares, solid lines*) incubated with increasing concentrations of compounds (0–100 μM) (n = 4 for each point) (*B*) AF568-actin (1 μM):C0-C2 (3 μM, *closed triangles, solid lines*) or AF568-actin (1 μM):phosphorylated (by PKA) C0-C2 (C0-C2P, 3 μM, *open triangles, dotted lines*), incubated with increasing amounts of 0-100 μM of suramin, (*C*) NF023, or (*D*) ATA (n = 2 from separate actin and C0-C2 preparations). Average and SE for each data point are shown. EC_{50} values for Actin + C0-C2 in panel *A* (*solid lines*) and Actin + phosphorylated C0-C2 in panels *B–D* (*dotted lines*) are listed in Table 1.

Table 1
Summary of Hit compound effects on the dose–response of AF568-actin-C0-C2 TR-F (left) and ITC (right) parameters of compound binding to C0-C2

	TR-F	TR-F	TR-F+PKA	TR-F+PKA	ITC	ITC	ITC	ITC	ITC
Compound	EC_{50} (μM)	n	EC_{50} (μM)	n	K_d (μM)	n	ΔH	ΔG	ΔS
Suramin	5.9 ± 1.2	3.6	4.8 ± 1.2	1.2	16.6 ± 1.0	3.4	−17.4	−26.8	32.3
NF023	16.3 ± 1.2	3.2	17.5 ± 11.8	1.8	42.0 ± 3.4	2.1	−30.2	−24.6	−19.2
ATA	7.9 ± 1.9	3.4	4.3 ± 0.9	1.4	25.9 ± 2.2	3.1	−10.2	−25.8	52.9

Average data are provided as mean ± SE and each experiment was done with two separate protein preparations. TR-F data is from Figure 3*A* measured at 2 μM C0-C2 and TR-F+PKA data is from Figure 3, *B–D* measured at 3 μM C0-C2.

ITC: compounds bind to C0-C2.

Potential binding of these three Hit compounds to cMyBP-C was evaluated by ITC. ITC titration curves of C0-C2 with each of the three identified compounds are shown in Figure 4, *A–C*. Very clear binding curves with saturation at an excess of C0-C2 indicate that there is direct interaction between the Hit compounds and C0-C2. Fitting the binding curves in Figure 4, *A–C* (and replicates done with a separate preparation of C0-C2) yielded dissociation constants of 15–75 μm and stoichiometries of C0-C2:compound of 1:2–3 (Table 1). For suramin, but not NF023 or ATA, weak interactions with actin alone (K_d=∼200 μM) were noted (Fig. S2).

TR-FRET: functional characterization of compounds on actin-cMyBP-C binding

Compound-induced changes in TR-F and ITC results showing direct binding of the Hit compounds to C0-C2 suggested that the Hit compounds bind to C0-C2, and this modulates its binding with actin. We attempted to confirm effects on binding using a standard cosedimentation assay where F-actin

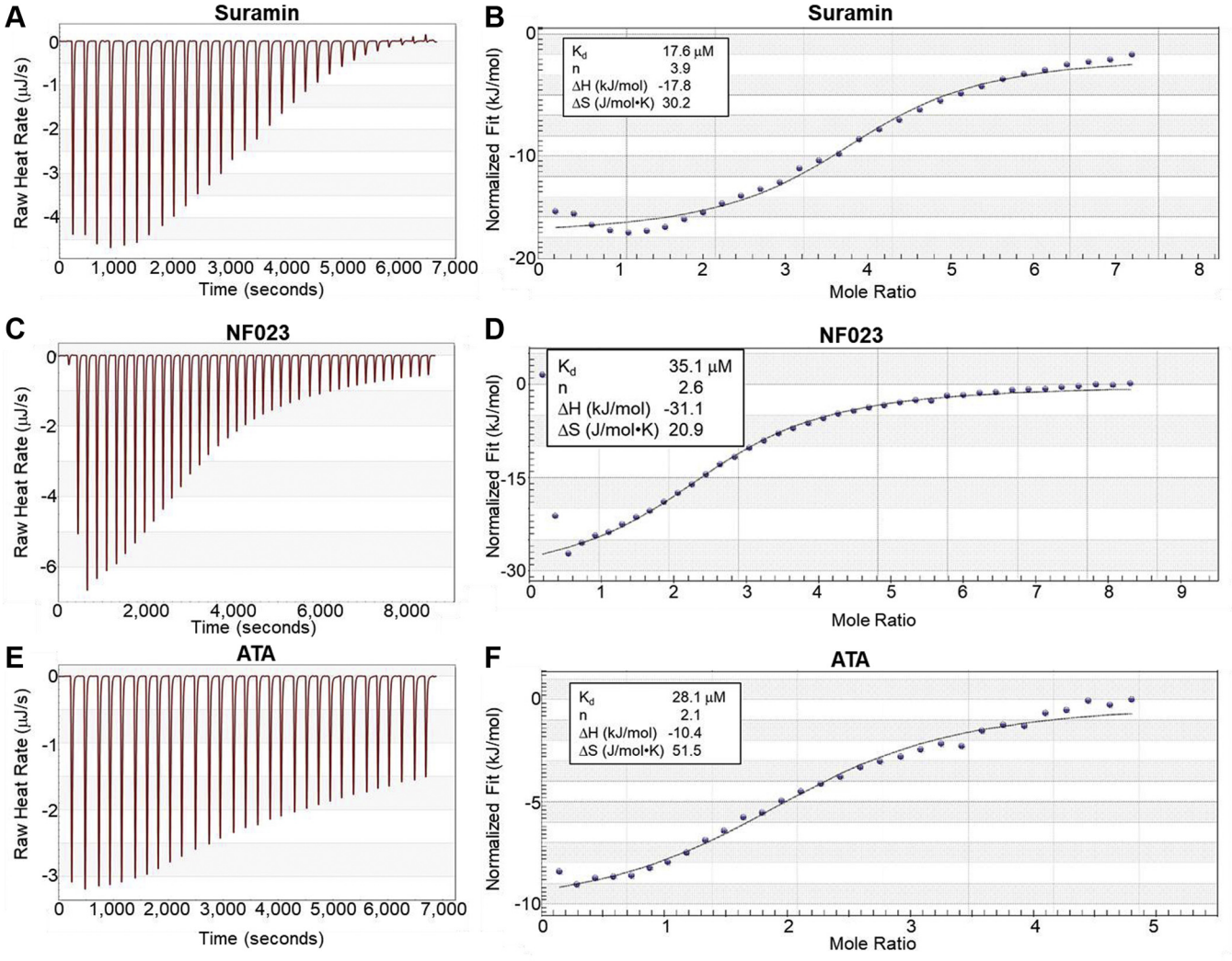

Figure 4. Isothermal titration calorimetry (ITC) of Hit compounds binding to C0-C2. *A,* titration of 100 μM C0-C2 (in 350 μl) with 30 2.5 μl injections of 3000 μM Suramin. *B*, fitted ITC binding curve for Suramin binding. *C* and *D*, the same for 2500 μM NF023 (40 injections). *E* and *F*, the same for 2000 μM ATA (30 injections). The binding of each Hit compound to C0-C2 is exothermic (ΔH < 0) and favorable reaction (ΔG < 0) (see Table 1).

was pelleted by centrifugation and the amount of C0-C2 bound to the F-actin in the pellet was quantitated. Unfortunately, all three Hit compounds caused C0-C2 to nonspecifically (in the absence of any actin) bind to the centrifuge tubes used for the assay. This was the case even though the tubes are precoated with BSA to prevent nonspecific sticking.

Since the compounds cause C0-C2 to bind nonspecifically to the centrifuge tube, we tested whether the compounds denature C0-C2 and cause it to become insoluble. We tested all three drugs for causing C0-C2 to aggregate by measuring absorbance in the visible range, beyond the absorption of protein or the drugs themselves. For suramin and NF023, we did not detect absorption, but for ATA we detected absorption (actually a reduction in transmitted light due to light scatter). This suggests that ATA causes some C0-C2 aggregation, which probably contributes to the background that interfered with our cosedimentation assay for this specific drug (Fig. S3).

As an alternative to cosedimentation, we performed an intermolecular FRET assay to follow C0-C2 binding to actin (Fig. 5*A*). Actin was labeled with the fluorescent donor fluorescein-5-maleimide (FMAL) and incubated with increasing concentrations of C0-C2 labeled with the acceptor tetramethylrhodamine (TMR) at amino acid Cys225 (see Experimental procedures) in the C1 domain. Binding of TMR-C0-C2 to FMAL-actin resulted in TR-FRET (Figs. 5*B* and S1*B*). TR-FRET binding curves for nonphosphorylated and phosphorylated C0-C2 showed that this TR-FRET was dose-dependent (Fig. 5*C*). These binding curves with K_d's around 1 and 3 μM are in good agreement with the TR-F-generated binding curves and those obtained by cosedimentation (15). At 1 μM FMAL-actin plus 2 μM TMR-C0-C2 (the same conditions as the original screen and for the dose–response curves in Fig. 3*A*), 20 μM suramin and ATA and 50 μM NF023 almost completely eliminated TR-FRET measured binding of both nonphosphorylated and phosphorylated C0-C2 (Fig. 5*D*).

TPA: characterization of Hit compounds' effects on actin structural dynamics

The three Hit compounds might interact directly with actin as well as with C0-C2. ITC showed only weak interaction of F-actin with suramin and no interaction with NF023 or ATA. We tested this further by monitoring compound effects on F-actin's structural dynamics by using TPA of actin labeled at Cys-374 with erythrosine iodoacetamide (ErIA) (Fig. 6*A*). None of the three compounds we identified in this screen affected actin's structural dynamics as measured by TPA. For comparison we show a fourth compound, GNF-5 that does bind actin and changes its anisotropy (Fig. 6*B*). This control

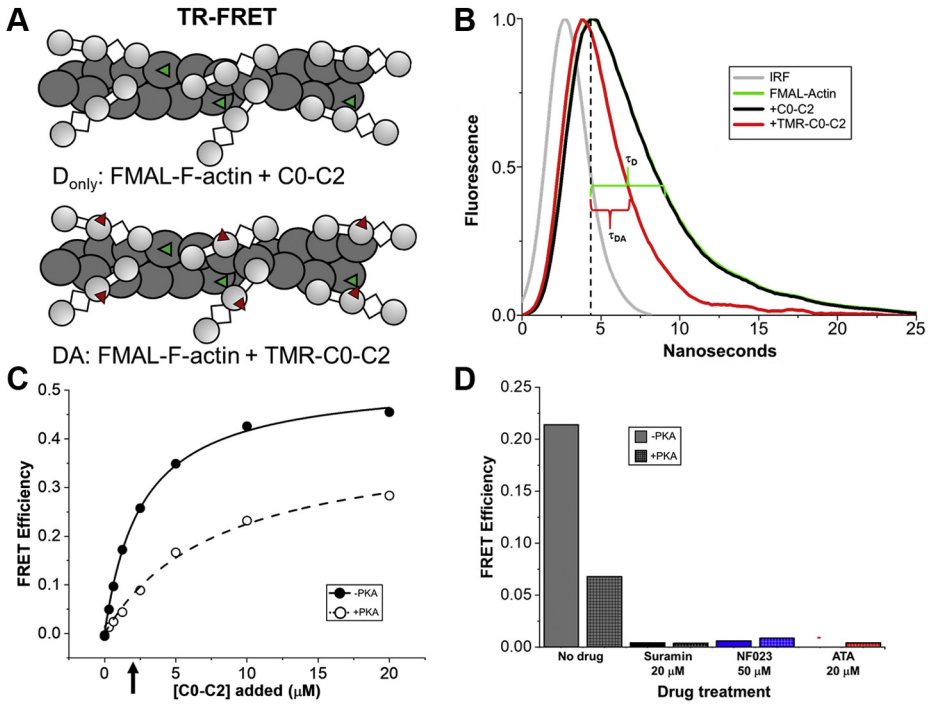

Figure 5. TR-FRET-binding curve of PKA and Hit compounds. ***A,*** cartoon depiction of F-actin labeled with FMAL (*green triangles*) bound to C0-C2 (unlabeled), the donor-only sample (D_{only}). Actin labeling is 10%; 1 FMAL for every ten actin monomers. And the same bound to C0-$C2^{Cys225}$ labeled with TMR (*red triangles*), the donor–acceptor sample (DA). *B*, fluorescence waveforms of FMAL-actin (*green line*) and the same in the presence of 20 μM C0-$C2^{Cys225}$ (*black line*) and 20 μM TMR-C0-$C2^{Cys225}$ (*red line*), all normalized to maximal fluorescence (waveforms without normalization can be found in Fig. S1*B*). Lifetime (τ) is the time at which the peak (*vertical dashed line*) fluorescence decays to ~0.37 (1/e). These times are indicated by the green bracket (τ_D = 4.2 ns for FMAL-actin with or without bound unlabeled C0-C2) and *red bracket* (τ_{DA} = 2.0 ns for FMAL-actin binding to TMR-C0-$C2^{Cys225}$). The instrument response function (IRF) is also shown (*gray line*). *C*, TR-FRET-based binding curve of 1 μM FMAL-actin and 0–20 μM TMR-C0-$C2^{Cys225}$ ±PKA. The concentration of C0-C2 (2 μM) used in the original screen and in testing of compound effects is indicated with an *arrow*. The K_d was 2.6 ± 0.1 μM for –PKA and 8 ± 1 μM for +PKA. *D*, effect of adding compounds to 1 μM FMAL-actin-2 μM TMR-C0-$C2^{Cys225}$ ±PKA (*arrow* in *C*). Compound concentrations are indicated. Aurintricarboxcylic acid (ATA) eliminated actin-C0-C2 FRET to near zero (*red* -). Data are means ± SE; however, errors are too small to be seen outside of the data points or bar borders. n = 9–10 for the binding curve and n = 4–10 for the compound tests from two separate actin and C0-C2 preparations. All values are the average ± SE.

was one of the compounds removed from the analysis due to effects on actin-alone in the screen.

This TPA assay was used to test the three Hit compounds for their ability to inhibit C0-C2 binding to actin. We previously showed that actin structural dynamics are restricted by C0-C2 binding (6, 7). Figure 6*C* shows the effect of C0-C2 binding on F-actin's final anisotropy (detecting rotational motions). Actin's final anisotropy was increased from 0.033 ± 0.001 to 0.071 ± 0.003 in the presence of C0-C2. Addition of the three Hit compounds completely removes the C0-C2 effects on F-actin anisotropy (returning to ∼0.033, Fig. 6, *C* and *D*), consistent with the compounds binding to C0-C2 and preventing it from binding to actin.

Discussion

The recently described TR-F assay, which monitors cMyBP-C's amino terminal C0-C2 domains binding to actin (15), successfully identified the first three compounds capable of inhibiting C0-C2 interactions with actin. Characterization of this inhibition using a new TR-FRET assay, ITC, and TPA indicates that these three compounds bind directly to C0-C2, inhibiting its ability to bind to actin. Thus, we have identified the first three cMyBP-C-binding compounds that decrease cMyBP-C's actin-binding function.

Three compounds from ∼1000 were reproducibly identified in two full screens of the LOPAC. That only three of the top 25 were reproducibly identified demonstrates the importance of replicate screening. Twenty two of the top preliminary hits in each screen did not show large effects in the other replicate screen and are considered false positives. In two additional screens of the same library, though not complete or optimal, the same three compounds, but no others, were found in the top 25 preliminary hits. We conclude that duplicate screening is necessary and sufficient for reliably identifying compounds using this screening technique. The reproducible Hit rate of ∼0.23% suggests that screening of larger libraries of compounds will yield a manageable number of compounds for further characterization.

Further characterization was needed to determine whether the identified compounds inhibit C0-C2–actin interactions by binding to one or both proteins. All three compounds were found to bind C0-C2 and not actin by using a combination of ITC, TR-FRET, and TPA assays.

ITC showed clear binding to C0-C2 in the absence of actin but did not demonstrate binding to actin at the appropriate concentration. K_d values determined for Hit compound binding were similar to the half-maximal inhibition values determined by dose–response curves using the original TR-F assay. The two assays showed a consistent ranking of activity with suramin>ATA>NF023 for binding and inhibition. The half-maximal inhibition values were roughly 2–3 times lower than the K_d values. We have not investigated this further but note that the n value of the ITC results (Table 1) suggests that 2–3 molecules of the compounds bind to each C0-C2. If inhibition is achieved by the binding of only one molecule of compound, this could explain the difference between the ITC K_d and TR-F half-maximal inhibition values. The ITC K_d

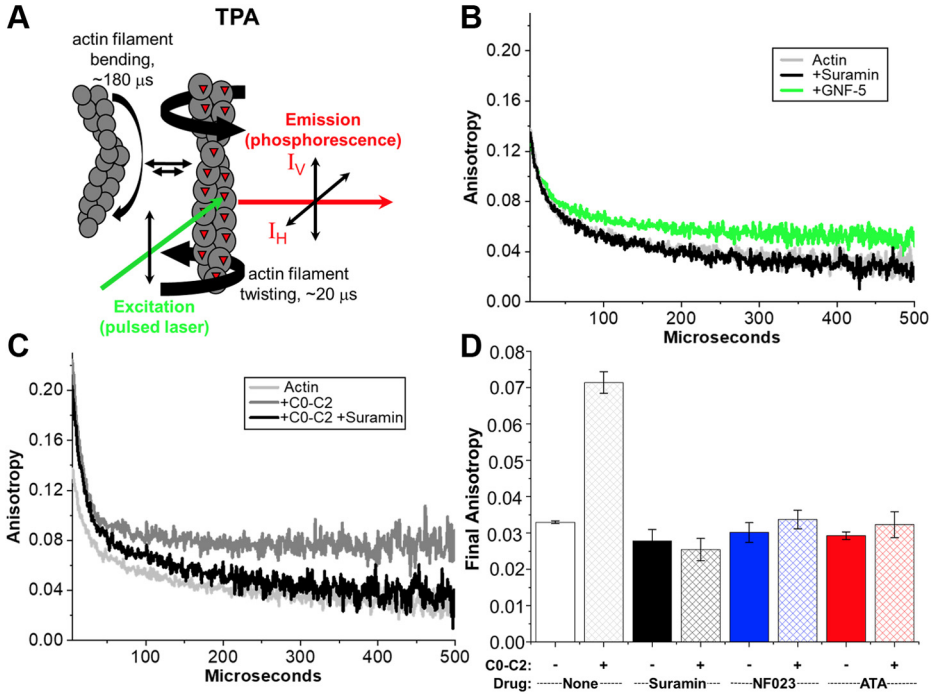

Figure 6. Effects of Hit compounds on actin rotational dynamics. *A*, schematic of transient phosphorescence anisotropy (TPA) measurement of actin labeled with erythrosine iodoacetamide (ErIA) where anisotropy of the emitted phosphorescence changes with the degree of actin filament twisting (from Bunch *et al.* (7)). *B*, TPA of ErIA-actin alone (*light gray*) +Suramin (*black*) or +GNF-5 (*green*). *C*, TPA of actin alone (*light gray*) actin+C0-C2 (*dark gray*) actin+C0-C2+Suramin (*black*). *D*, effects of Hit compounds on TPA of actin (*solid bars*) or actin+C0-C2 (*criss-cross bars*). Compounds were present at 20 μM for Suramin and ATA and 50 μM for NF023.

values would represent an average K_d of multiple binding interactions with each C0-C2, whereas the TR-F half maximal inhibition values may be dependent on only the single highest affinity site being occupied to prevent actin binding. Alternatively, there may be a higher affinity of the drugs for C0-C2 bound to actin (TR-F half maximal inhibition values) than for free C0-C2 in solution (ITC).

Adding a FRET acceptor (TMR) to C0-C2 allowed us to monitor its interaction with F-actin labeled with donor (FMAL) by TR-FRET. Using this new assay, we were able to observe the anticipated reduced binding when C0-C2 was phosphorylated with PKA. This assay confirmed the TR-F results, showing dramatic reduction of nonphosphorylated or phosphorylated C0-C2-actin interactions by all three compounds. Use of conventional cosedimentation assays to confirm binding was hindered by the compounds causing high background values, as they either promoted a small amount of C0-C2 aggregation (ATA) or promoted C0-C2 binding to the tubes used in this assay (suramin and NF023).

In addition to ITC, we assayed interactions of the three compounds with actin using TPA. None of the three compounds altered actin's anisotropy, suggesting that they were not binding to actin. C0-C2 binding to F-actin increased its anisotropy as expected and all three compounds prevented this. This further confirmed that the compound effects were due to their binding to C0-C2 and preventing its binding to actin. This result contrasts with our results screening for compounds that modulate actin–myosin interactions (31), where most of the identified compounds had a direct impact on the TPA of actin alone.

Compounds binding to cardiac MyBP-C but not to actin may be expected to have fewer side effects than those binding to the very well-conserved actin present in all cells. It will be important to determine whether these (and future) compounds that bind to cardiac MyBP-C also bind to skeletal MyBP-C. The observations from ITC that these compounds may bind to C0-C2 in a 2–3:1 ratio suggest that they bind to multiple MyBP-C domains such as C0, C1, and C2. Finally, it will be important to characterize the compounds' effects on C0-C2 binding to myosin.

Much remains to be learned about the effects of these compounds on cardiac muscle contractility, but the approach used in this work clearly indicates that the TR-F assay is suitable for screening thousands of compounds to identify cMyBP-C-binding Hits capable of altering its function. We now have, for the first time, a validated HTS focused on cMyBP-C, a known key factor in heart failure.

The promising results from this screen suggest that similar screens using regulated thin filaments (containing tropomyosin and troponin) should be feasible. In our earlier work we observed that tropomyosin alone increased C0-C2 binding and TR-F effects, as predicted from structural studies (5, 15). Compounds capable of modifying C0-C2 interactions with tropomyosin (in the presence or absence of troponin) may be identified in these future screens. Finally, similar high-throughput assays, based on lifetime changes of probes attached to myosin (the other recognized C0-C2 binding protein) should be feasible, and we are currently pursuing this.

Experimental procedures

Actin preparations and labeling

Actin was prepared from rabbit skeletal muscle by extracting acetone powder in cold water as described in Bunch *et al.* (32).

For TR-F experiments, actin was labeled at Cys-374 with Alexa Fluor 568 C_5 maleimide (AF568, Thermo Fisher Scientific) and in preliminary experiments with Alexa Fluor 546 C_5 maleimide (AF546). Labeling was done on F-actin. To 50 μM of G-actin in G-buffer (10 mM Tris pH 7.5, 0.2 mM $CaCl_2$, 0.2 mM ATP), Tris pH 7.5 was added to a final concentration of 20 mM and actin was then polymerized by the addition of 3 M KCl (to a final concentration of 100 mM) and 0.5 M $MgCl_2$ (to a final concentration of 2 mM), followed by incubation at 23 °C for 1 h. AF568 was added to a final concentration of 50–100 μM (from a 20 mM stock in DMF). Labeling was done for 1 h at 23 °C and then overnight at 4 °C. For the experiments shown in Figure 2*D*, AF568 labeling in three separate actin preparations was 65%, 40%, and 34% ([dye]/[actin]). For AF546, labeling was 87% and 28% (two separate preparations tested). TR-F effects were the same at all labeling levels and the results were combined. For TR-FRET experiments, actin was similarly labeled with fluorescein-5-maleimide (FMAL). Labeling with FMAL was done at a final FMAL concentration of 1 mM for 5 h at 23 °C and then overnight at 4 °C. Labeling was stopped by the addition of a 5-fold molar excess of DTT. Unincorporated dye (AF568 or FMAL) was removed by cycling the actin through F-actin and G-actin states as described in (15). For FMAL-labeled actin, to avoid TR-FRET between FMAL on neighboring Cys-374 residues of actin monomers in F-actin, unlabeled G-actin was mixed with FMAL-actin to achieve 10% FMAL-actin prior to the final actin polymerization. For phosphorescence experiments (TPA), actin was labeled at Cys-374 with erythrosin-5′-iodoacetamide (ErIA; AnaSpec) (6, 33). The degree of labeling by ErIA was 83% and 42% dye/C0-C2 as measured by UV-vis absorbance. Fluorescent and phosphorescent labeled F-actins were stabilized by the addition of equimolar phalloidin.

For all assays F-actin was resuspended in and/or dialyzed against MOPS-actin-binding buffer, M-ABB (100 mM KCl, 10 mM MOPS pH 6.8, 2 mM $MgCl_2$, 0.2 mM $CaCl_2$, 0.2 mM ATP, 1 mM DTT).

Recombinant human cMyBP-C fragment preparations and labeling

pET45b vectors encoding *E. coli* optimized codons for the C0-C2 portion of human cMyBP-C with N-terminal 6x His tag and TEV protease cleavage site were obtained from GenScript. For TR-FRET-binding assays, we mutated C0-C2 so that it contained a single cysteine at position 225, a surface-exposed residue in the C1 domain. To achieve this, the five endogenous cysteines in C0-C2 were mutated to amino acids found in other MyBP-C proteins at analogous positions (C239L, C249S, C426T, C436V, and C443S) and then His-225 was mutated to Cys, termed C0-C2^{Cys225}. Mutations were engineered in the human cMyBP-C C0-C2 using a Q5 Site-Directed Mutagenesis Kit (New England Bio Labs). All sequences were confirmed by

DNA sequencing (Eton Biosciences). Protein production in *E. coli* BL21DE3-competent cells (New England Bio Labs) and purification of C0-C2 protein using His60 Ni Superflow resin were done as described (32). C0-C2 (with His-tag removed by TEV protease digestion) was further purified using size-exclusion chromatography to achieve >90% intact C0-C2 as described (7) and then concentrated, dialyzed to 50/50 buffer (50 mM NaCl and 50 mM Tris, pH 7.5), and stored at 4 °C.

For TR-FRET experiments, C0-C2^{Cys225} was labeled with tetramethylrhodamine (TMR) in 50/50 buffer. C0-C2^{Cys225} (50 μM) was first treated with the reducing agent TCEP (200 μM) for 30 min at 23 °C, and then TMR was added (from a 20 mM stock in DMF) to a final concentration of 200 μM. Labeling was done for 1 h at 23 °C and terminated by the addition DTT (to 1 mM). Unincorporated dye was removed by extensive dialysis against M-ABB buffer. The degree of labeling was 95% dye/C0-C2 as measured by UV-vis absorbance.

In vitro *phosphorylation of cMyBP-C*

C0-C2 was treated with 7.5 ng PKA/μg C0-C2 at 30 °C for 30 min. This is 3x the level (2.5 ng PKA/μg C0-C2) needed to achieve maximal phosphorylation as determined by in-gel staining of proteins with Pro-Q Diamond (7, 15).

Fluorescence data acquisition

Fluorescence lifetime measurements were acquired using a high-precision fluorescence lifetime plate reader (FLTPR; Fluorescence Innovations, Inc) (32, 34), provided by Photonic Pharma LLC. For TR-F experiments, AF568 (or AF546)-labeled F-actin (alone or mixed with C0-C2) was excited with a 532-nm microchip laser (Teem Photonics) and emission was filtered with a 586/20-nm band-pass filter (Semrock). For TR-FRET experiments, FMAL was excited with a 473-nm microchip laser (Bright Solutions) and emission was filtered with 488-nm long-pass and 517/20-nm band-pass filters (Semrock). The photomultiplier tube (PMT) voltage was adjusted so that the peak signals of the instrument response function (IRF) and the TR-F biosensor were similar. The observed TR-F waveform was analyzed as described previously (15, 35).

LOPAC library screen

The 1280 LOPAC compounds were received in 96-well plates (LOPAC^{1280}, Sigma-Aldrich) and were reformatted into 1536-well flat, black-bottom polypropylene plates (Greiner Bio-One). In total, 50 nl of compounds was dispensed using an automated Echo 550 acoustic liquid dispenser (Labcyte). LOPAC compounds were formatted into plates, with the first two and last two columns loaded with 50 nl of DMSO and used for compound-free controls. The final concentration of the compounds was 10 μM. These assay plates were then heat-sealed using a PlateLoc Thermal Microplate Sealer (Agilent Technologies) and stored at −20 °C. Before screening, compound plates were equilibrated to room temperature (25 °C). In total, 1 μM AF568-labeled actin without or with 2 μM C0-C2 in M-ABB was dispensed by a Multidrop Combi Reagent Dispenser (Thermo Fisher Scientific) into the 1536-well assay plates containing the compounds. Plates were incubated at room temperature for 20 min before recording the data with the FLTPR. Plates were rescanned after 120 min incubation.

Two full screens were done using different batches of AF568-labeled actin, C0-C2, and test compounds. Two additional suboptimal (due to liquid dispensing errors that necessitated removing 191 samples from the analysis, and a batch of AF568-actin that showed lower than expected lifetime changes with the binding of C0-C2 in the absence of compounds) screens were included in the analysis (Tables S3 and S4) as they yielded complementary results.

TR-F and HTS data analysis

Following data acquisition, TR-F waveforms observed for each well were convolved with the IRF to determine the lifetime (τ) (Equation 1) by fitting to a single-exponential decay (15, 35).

The decay of the excited state of the fluorescent dye attached to actin at Cys-374 to the ground state is:

$$F(t) = I_0 \exp(-t/\tau) \quad (1)$$

where I_0 is the fluorescence intensity upon peak excitation (t = 0), and τ is the fluorescence lifetime (t = τ when I decays to 1/e or ∼37% of I_0).

TR-F assay quality was determined from controls (DMSO-only samples) on each plate as indexed by the Z' factor. A value of 0.5–1 indicates excellent assay quality while 0.0–0.5 indicates a doable assay quality (15, 36, 37):

$$Z' = 1 - \frac{3(\sigma_0 + \sigma)}{|\mu_0 - \mu|} \quad (2)$$

where σ_0 and σ are the SD of the controls τ_0 and τ, respectively, and μ_0 and μ are the means of the controls τ_0 and τ, respectively. Here, the two-sample comparison was AF568-actin with DMSO (τ_0) *versus* AF568-actin with C0-C2 and DMSO (τ).

A compound was considered a Hit if it was in the top 25 compounds in each of two independent screenings of the LOPAC. Top compounds were those that increased the lifetime of AF568-actin when C0-C2 was present (indicating inhibition of C0-C2 binding). Compounds that altered AF568-actin lifetime when C0-C2 was not present by >4 SD relative to that of the control samples (those exposed to 0.1% DMSO) were first removed from the analysis. This resulted in the removal, from analysis, of 210 compounds from the first screen and 106 compounds from the second screen. Any change in lifetime induced by a compound on AF568-actin alone was then subtracted from the effect of the compound on AF568-actin when C0-C2 was present. The resulting C0-C2-dependent change for all compounds was ranked.

TR-F concentration–response assay

The Hit compounds were dissolved in DMSO to make a 10 mM stock solution, which was serially diluted in 96-well mother plates. Hits were screened at eight concentrations (0.5–100 μM). Compounds (1 μl) were transferred from the mother plates into 384-well plates using a Mosquito HV liquid handler (TTP Labtech Ltd). The same procedure of dispensing as for the pilot screening was applied in the TR-F concentration–response assays. Concentration dependence of the TR-F change was fitted using the Hill equation (38):

$$\tau = \tau_o + \frac{\tau_{max} C^{\alpha}}{EC_{50}^{\alpha} + C^{\alpha}} \quad (3)$$

where τ and τ_0 are TR-F in the presence and in the absence of the compound, τ_{max} is the maximum effect, C is the compound concentration, EC_{50} is the compound concentration for which 50% of maximum effect is obtained, and α is the Hill coefficient of sigmoidicity.

Isothermal titration calorimetry (ITC)

The titration of compounds binding to cMyBP-C was performed on an Affinity ITC (TA Instruments). Each compound in M-ABB buffer (2000–3000 μM) was titrated into C0-C2 in M-ABB buffer (100 μM, 350 μl). For the titration, a preliminary 2.5-μl injection (ignored in data analysis) was followed by 19–39 subsequent 2.5-μl injections with 4 min waits between each injection. The reference cell was filled with distilled water. To account for heat changes of dilution and mechanical mixing, binding data were corrected by subtraction of the final plateau injection values (when binding is complete) prior to curve fitting. Corrected binding data was processed using the NanoAnalyze analysis software (TA Instruments).

FMAL-actin-TMR-C0-C2 TR-FRET binding assay

In total, 1 μM F-Actin labeled (to 10%) on Cys-374 with FMAL (donor fluor) was incubated with increasing concentrations (0–20 μM) of C0-$C2^{Cys225}$ unlabeled (for donor only (D) data acquisition) or labeled to 95% with TMR (acceptor fluor) (for donor–acceptor (DA) data). Lifetimes of FMAL-actin were determined for D and DA at each concentration of C0-$C2^{Cys225}$. TR-FRET efficiency ($1 - (\tau_{DA}/\tau_D)$) was determined for each C0-$C2^{Cys225}$ concentration. The binding curve was generated from data from two separate preparations of actin and C0-$C2^{Cys225}$. Testing of compound effects by TR-FRET was similarly done at 1 μM FMAL-actin with unlabeled C0-$C2^{Cys225}$ (D) and TMR-C0-$C2^{Cys225}$ (DA), both at 2 μM.

Transient phosphorescence anisotropy (TPA)

Phalloidin-stabilized ErIA-actin was prepared and diluted in M-ABB to 1 μM alone or in combination with each compound at concentrations that first exhibited maximal effect in the initial TR-F assay; 20 μM for suramin and ATA and 50 μM for NF023. The same mixtures were tested in the presence of 2 μM C0-C2. These were added together with glucose catalase/oxidase to prevent photobleaching, and TPA was performed at 25 °C to determine anisotropy values (7).

Visible light scattering

All three drugs were tested for causing C0-C2 to aggregate by measuring absorbance in the visible range beyond the absorption of protein or the drugs themselves. Observed absorbance in these wavelengths is actually loss of transmitted light due to light scattering from aggregated C0-C2. 2 or 10 μM of C0-C2 was mixed with 20 μM of suramin, NF023, or ATA for 20 min and wavelengths 250–600 nm were scanned using a Beckman Coulter DU730 UV/Vis Spectrophotometer to determine optical density. The same was done with 2 or 10 μM of C0-C2 and 20 μM of suramin, NF023, or ATA alone.

Statistics

Average data are provided as mean ± standard error (SE) and each experiment was done with two separate protein preparations.

Data availability

All data discussed are presented within the article.

Supporting information—This article contains supporting information.

Acknowledgments—We thank Samantha Yuen (UMN) for technical assistance with the fluorescence lifetime plate reader.

Author contributions—T. A. B., P. G., D. D. T., and B. A. C. conceptualization; T. A. B., P. G., V. C. L., A. R. T., A. W., and B. A. C. formal analysis; T. A. B., P. G., D. D. T., and B. A. C. supervision; T. A. B., P. G., V. C. L., and B. A. C. validation; T. A. B., P. G., D. D. T., V. C. L., A. R. T., R.-S. K., A. W., and B. A. C. investigation; T. A. B., P. G., D. D. T., and B. A. C. visualization; T. A. B., P. G., V. C. L., R.-S. K., D. D. T., and B. A. C. methodology; T. A. B., P. G., D. D. T., and B. A. C. writing-original draft; T. A. B., P. G., V. C. L., A. R. T., R.-S. K., A. W., D. D. T., and B. A. C. writing-review and editing; V. C. L. and B. A. C. project administration; D. D. T. and B. A. C. funding acquisition; B. A. C. resources.

Funding and additional information—This work was supported by National Institutes of Health grants R37 AG26160 (to D. D. T.) and R01 HL141564 (to B. A. C.) and a University of Arizona Sarver Heart Center "Novel Research Project Award in the Area of Cardiovascular Disease and Medicine" (to B. A. C). The content is solely the responsibility of the authors and does not necessarily represent the official views of the National Institutes of Health.

Conflict of interest—D. D. T. holds equity in and serves as President of Photonic Pharma LLC. This relationship has been reviewed and managed by the University of Minnesota. Photonic Pharma had no role in this study, except to provide some instrumentation, as stated in Experimental procedures. B. A. C. filed a PCT patent application based on this work (patent pending, serial no. PCT/US21/14142). The other authors declare no competing financial interests.

Abbreviations—The abbreviations used are: AF546, Alexa Fluor 546; AF568, Alexa Fluor 568; ATA, aurintricarboxylic acid; B_{max},

maximum molar binding ratio; BSA, bovine serum albumin; C0-C2, N-terminal fragment of cMyBP-C comprised of C0-P/A-C1-M-C2 domains and linkers; cMyBP-C, cardiac myosin-binding protein C; DA, donor plus acceptor; DCM, dilated cardiomyopathy; DMF, dimethylformamide; DMSO, dimethylsulphoxide; DO, donor only; DTT, dithiothreitol; DWR, direct waveform recording; ErIA, erythrosine iodoacetamide phosphorescent dye; F-actin, filamentous actin; FLTPR, fluorescence lifetime plate reader; FMAL, fluorescein-5-maleimide; HCM, hypertrophic cardiomyopathy; HTS, high-throughput screen; IAEDANS, 5-((((2-iodoacetyl)amino)ethyl) amino)naphtalene-1-sulfonic acid; ITC, isothermal titration calorimetry; K_d, dissociation constant; LOPAC, library of pharmacologically active compounds; M, M-domain, phosphorylatable linker between C1 and C2; M-ABB, MOPS-actin binding buffer; P/A, proline/alanine-rich linker between domains C0 and C1; G-actin, globular actin; TCEP, tris(2-carboxyethyl)phosphine; TPA, transient phosphorescence anisotropy; TMR, tetramethylrhodamine; TR-F, time-resolved fluorescence; TR-FRET, time-resolved fluorescence energy transfer; PKA, protein kinase A; SD, standard deviations; SE, standard errors.

References

1. Spudich, J. A. (2019) Three perspectives on the molecular basis of hypercontractility caused by hypertrophic cardiomyopathy mutations. *Pflugers Arch.* **471**, 701–717
2. Arimura, T., Ishikawa, T., Nunoda, S., Kawai, S., and Kimura, A. (2011) Dilated cardiomyopathy-associated BAG3 mutations impair Z-disc assembly and enhance sensitivity to apoptosis in cardiomyocytes. *Hum. Mutat.* **32**, 1481–1491
3. Hershberger, R. E., Hedges, D. J., and Morales, A. (2013) Dilated cardiomyopathy: The complexity of a diverse genetic architecture. *Nat. Rev. Cardiol.* **10**, 531–547
4. Mun, J. Y., Previs, M. J., Yu, H. Y., Gulick, J., Tobacman, L. S., Beck Previs, S., Robbins, J., Warshaw, D. M., and Craig, R. (2014) Myosin-binding protein C displaces tropomyosin to activate cardiac thin filaments and governs their speed by an independent mechanism. *Proc. Natl. Acad. Sci. U. S. A.* **111**, 2170–2175
5. Risi, C., Belknap, B., Forgacs-Lonart, E., Harris, S. P., Schroder, G. F., White, H. D., and Galkin, V. E. (2018) N-terminal domains of cardiac myosin binding protein C cooperatively activate the thin filament. *Structure* **26**, 1604–1611.e1604
6. Colson, B. A., Rybakova, I. N., Prochniewicz, E., Moss, R. L., and thomas, D. D. (2012) Cardiac myosin binding protein-C restricts intrafilament torsional dynamics of actin in a phosphorylation-dependent manner. *Proc. Natl. Acad. Sci. U. S. A.*
7. Bunch, T. A., Kanassatega, R. S., Lepak, V. C., and Colson, B. A. (2019) Human cardiac myosin-binding protein C restricts actin structural dynamics in a cooperative and phosphorylation-sensitive manner. *J. Biol. Chem.* **294**, 16228–16240
8. Walcott, S., Docken, S., and Harris, S. P. (2015) Effects of cardiac Myosin binding protein-C on actin motility are explained with a drag-activation-competition model. *Biophys. J.* **108**, 10–13
9. Wang, C., Schwan, J., and Campbell, S. G. (2016) Slowing of contractile kinetics by myosin-binding protein C can be explained by its cooperative binding to the thin filament. *J. Mol. Cell Cardiol.* **96**, 2–10
10. Robinett, J. C., Hanft, L. M., Geist, J., Kontrogianni-Konstantopoulos, A., and McDonald, K. S. (2019) Regulation of myofilament force and loaded shortening by skeletal myosin binding protein C. *J. Gen. Physiol.* **151**, 645–659
11. Pohlmann, L., Kroger, I., Vignier, N., Schlossarek, S., Kramer, E., Coirault, C., Sultan, K. R., El-Armouche, A., Winegrad, S., Eschenhagen, T., and Carrier, L. (2007) Cardiac myosin-binding protein C is required for complete relaxation in intact myocytes. *Circ. Res.* **101**, 928–938
12. McNamara, J. W., Li, A., Smith, N. J., Lal, S., Graham, R. M., Kooiker, K. B., van Dijk, S. J., Remedios, C. G., Harris, S. P., and Cooke, R. (2016) Ablation of cardiac myosin binding protein-C disrupts the super-relaxed state of myosin in murine cardiomyocytes. *J. Mol. Cell Cardiol.* **94**, 65–71
13. Nag, S., Trivedi, D. V., Sarkar, S. S., Adhikari, A. S., Sunitha, M. S., Sutton, S., Ruppel, K. M., and Spudich, J. A. (2017) The myosin mesa and the basis of hypercontractility caused by hypertrophic cardiomyopathy mutations. *Nat. Struct. Mol. Biol.* **24**, 525–533
14. Shaffer, J. F., Kensler, R. W., and Harris, S. P. (2009) The myosin-binding protein C motif binds to F-actin in a phosphorylation-sensitive manner. *J. Biol. Chem.* **284**, 12318–12327
15. Bunch, T. A., Lepak, V. C., Bortz, K. M., and Colson, B. A. (2021) A high-throughput fluorescence lifetime-based assay for detecting binding of myosin-binding protein C to F-actin. *J. Gen. Physiol.* **153**, e202012707
16. Gruen, M., Prinz, H., and Gautel, M. (1999) cAPK-phosphorylation controls the interaction of the regulatory domain of cardiac myosin binding protein C with myosin-S2 in an on-off fashion. *FEBS Lett.* **453**, 254–259
17. Gruen, M., and Gautel, M. (1999) Mutations in beta-myosin S2 that cause familial hypertrophic cardiomyopathy (FHC) abolish the interaction with the regulatory domain of myosin-binding protein-C. *J. Mol. Biol.* **286**, 933–949
18. Previs, M. J., Prosser, B. L., Mun, J. Y., Previs, S. B., Gulick, J., Lee, K., Robbins, J., Craig, R., Lederer, W. J., and Warshaw, D. M. (2015) Myosin-binding protein C corrects an intrinsic inhomogeneity in cardiac excitation-contraction coupling. *Sci. Adv.* **1**, e1400205
19. Weith, A., Sadayappan, S., Gulick, J., Previs, M. J., Vanburen, P., Robbins, J., and Warshaw, D. M. (2012) Unique single molecule binding of cardiac myosin binding protein-C to actin and phosphorylation-dependent inhibition of actomyosin motility requires 17 amino acids of the motif domain. *J. Mol. Cell. Cardiol.* **52**, 219–227
20. Rosas, P. C., Liu, Y., Abdalla, M. I., Thomas, C. M., Kidwell, D. T., Dusio, G. F., Mukhopadhyay, D., Kumar, R., Baker, K. M., Mitchell, B. M., Powers, P. A., Fitzsimons, D. P., Patel, B. G., Warren, C. M., Solaro, R. J., *et al.* (2015) Phosphorylation of cardiac Myosin-binding protein-C is a critical mediator of diastolic function. *Circ. Heart Fail.* **8**, 582–594
21. McNamara, J. W., Singh, R. R., and Sadayappan, S. (2019) Cardiac myosin binding protein-C phosphorylation regulates the super-relaxed state of myosin. *Proc. Natl. Acad. Sci. U. S. A.* **116**, 11731–11736
22. Colson, B. A., Thompson, A. R., Espinoza-Fonseca, L. M., and Thomas, D. D. (2016) Site-directed spectroscopy of cardiac myosin-binding protein C reveals effects of phosphorylation on protein structural dynamics. *Proc. Natl. Acad. Sci. U. S. A.* **113**, 3233–3238
23. Previs, M. J., Mun, J. Y., Michalek, A. J., Previs, S. B., Gulick, J., Robbins, J., Warshaw, D. M., and Craig, R. (2016) Phosphorylation and calcium antagonistically tune myosin-binding protein C's structure and function. *Proc. Natl. Acad. Sci. U. S. A.* **113**, 3239–3244
24. Jacques, A. M., Copeland, O., Messer, A. E., Gallon, C. E., King, K., McKenna, W. J., Tsang, V. T., and Marston, S. B. (2008) Myosin binding protein C phosphorylation in normal, hypertrophic and failing human heart muscle. *J. Mol. Cell Cardiol.* **45**, 209–216
25. Copeland, O., Sadayappan, S., Messer, A. E., Steinen, G. J., van der Velden, J., and Marston, S. B. (2010) Analysis of cardiac myosin binding protein-C phosphorylation in human heart muscle. *J. Mol. Cell. Cardiol.* **49**, 1003–1011
26. Malik, F. I., Hartman, J. J., Elias, K. A., Morgan, B. P., Rodriguez, H., Brejc, K., Anderson, R. L., Sueoka, S. H., Lee, K. H., Finer, J. T., Sakowicz, R., Baliga, R., Cox, D. R., Garard, M., Godinez, G., *et al.* (2011) Cardiac myosin activation: A potential therapeutic approach for systolic heart failure. *Science* **331**, 1439–1443
27. Green, E. M., Wakimoto, H., Anderson, R. L., Evanchik, M. J., Gorham, J. M., Harrison, B. C., Henze, M., Kawas, R., Oslob, J. D., Rodriguez, H. M., Song, Y., Wan, W., Leinwand, L. A., Spudich, J. A., McDowell, R. S., *et al.* (2016) A small-molecule inhibitor of sarcomere contractility suppresses hypertrophic cardiomyopathy in mice. *Science* **351**, 617–621
28. Cornea, R. L., Gruber, S. J., Lockamy, E. L., Muretta, J. M., Jin, D., Chen, J., Dahl, R., Bartfai, T., Zsebo, K. M., Gillispie, G. D., and Thomas, D. D. (2013) High-throughput FRET assay yields allosteric SERCA activators. *J. Biomol. Screen* **18**, 97–107

29. Schaaf, T. M., Li, A., Grant, B. D., Peterson, K., Yuen, S., Bawaskar, P., Kleinboehl, E., Li, J., Thomas, D. D., and Gillispie, G. D. (2018) Red-shifted FRET biosensors for high-throughput fluorescence lifetime screening. *Biosensors (Basel)* **8**
30. Simeonov, A., Jadhav, A., Thomas, C. J., Wang, Y., Huang, R., Southall, N. T., Shinn, P., Smith, J., Austin, C. P., Auld, D. S., and Inglese, J. (2008) Fluorescence spectroscopic profiling of compound libraries. *J. Med. Chem.* **51**, 2363–2371
31. Guhathakurta, P., Prochniewicz, E., Grant, B. D., Peterson, K. C., and Thomas, D. D. (2018) High-throughput screen, using time-resolved FRET, yields actin-binding compounds that modulate actin-myosin structure and function. *J. Biol. Chem.* **293**, 12288–12298
32. Bunch, T. A., Lepak, V. C., Kanassatega, R. S., and Colson, B. A. (2018) N-terminal extension in cardiac myosin-binding protein C regulates myofilament binding. *J. Mol. Cell Cardiol.* **125**, 140–148
33. Prochniewicz, E., Walseth, T. F., and Thomas, D. D. (2004) Structural dynamics of actin during active interaction with myosin: Different effects of weakly and strongly bound myosin heads. *Biochemistry* **43**, 10642–10652
34. Schaaf, T. M., Peterson, K. C., Grant, B. D., Bawaskar, P., Yuen, S., Li, J., Muretta, J. M., Gillispie, G. D., and Thomas, D. D. (2017) High-throughput spectral and lifetime-based FRET screening in living cells to identify small-molecule effectors of SERCA. *SLAS Discov.* **22**, 262–273
35. Gruber, S. J., Cornea, R. L., Li, J., Peterson, K. C., Schaaf, T. M., Gillispie, G. D., Dahl, R., Zsebo, K. M., Robia, S. L., and Thomas, D. D. (2014) Discovery of enzyme modulators via high-throughput time-resolved FRET in living cells. *J. Biomol. Screen* **19**, 215–222
36. Rebbeck, R. T., Essawy, M. M., Nitu, F. R., Grant, B. D., Gillispie, G. D., Thomas, D. D., Bers, D. M., and Cornea, R. L. (2017) High-throughput screens to discover small-molecule modulators of ryanodine receptor calcium release channels. *SLAS Discov.* **22**, 176–186
37. Zhang, J. H., Chung, T. D., and Oldenburg, K. R. (1999) A simple statistical parameter for use in evaluation and validation of high throughput screening assays. *J. Biomol. Screen* **4**, 67–73
38. Goutelle, S., Maurin, M., Rougier, F., Barbaut, X., Bourguignon, L., Ducher, M., and Maire, P. (2008) The Hill equation: A review of its capabilities in pharmacological modelling. *Fundam. Clin. Pharmacol.* **22**, 633–648